Simulating Liquid Crystals

Kit Gallagher *Supervisors: Prof Erika Eiser, Mr Jiaming Yu*

March 21, 2021

This document is simply to give an overview of methods used and data obtained in the project. It is likely that many of the methods and results detailed here will be used in the final report, but this is not intended to be a full report; rather a collection of ideas that can be used in the writing of this final report.

1 Methods

1.1 Order Parameter

"*The description of liquid crystals involves an analysis of order. A second rank symmetric traceless tensor order parameter is used to describe the orientational order of a nematic liquid crystal, although a scalar order parameter is usually sufficient to describe uniaxial nematic liquid crystals. To make this quantitative, an orientational order parameter is usually defined based on the average of the second Legendre polynomial:*

$$S = \langle P_2(\cos\theta)\rangle = \left\langle \frac{3\cos^2(\theta) - 1}{2} \right\rangle \tag{1}$$

where θ is the angle between the liquid-crystal molecular axis and the local director (which is the 'preferred direction' in a volume element of a liquid crystal sample, also representing its local optical axis)." - Copied from wiki

However, in our case the local director is not known, and so I have approximated it as the mean director averaged across all particles. Eppenga et al. [1] suggest an alternative method, for when this local director is not known.

In summary they express this order parameter through the tensor **Q**, where the largest eigenvalue corresponds to the traditional eigenvalue. This is conveniently done by finding the eigenvalues of tensor M, which shares eigenvectors with Q and has eigenvectors which can be related to those of Q. Figure 2A in this paper shows the relationship between the ideal order parameter and the largest eigenvalue; there is very good agreement beyond very small values, and so this is clearly sufficient to approximate the true order parameter. Mathematical details of this may be included in an appendix?

2 Results

2.1 Square Simulation Region

This section details the results from my first long simulation to achieve nematic phase formation. This simulation took three hours to run, and consisted of 6 shrinking stages (each of 50,000 steps), with

1,000,000 simulation steps between each one. It had 1000 particles inside a cubic box, of initial side length 10 times greater than the length of one nanoparticle. The final side length of the box was 2.5 times greater than the length of one nanoparticle, with a final volume fraction within the box of X%.

After the penultimate shrinking step, a phase transition was observed from the disordered isotropic phase to an ordered nematic phase, as depicted in Figure 1. This is characterised by orientational order (ie particles tend to have similar orientations), while having no long range positional order (ie the centres of mass of each particle are randomly distributed through space). This can be observed easily in Figure 1b, where particle ordering can be easily observed on the top and right hand faces. Note that each molecule is artificially given a different colour to aid recognition of them; this does not have any physical relevance.

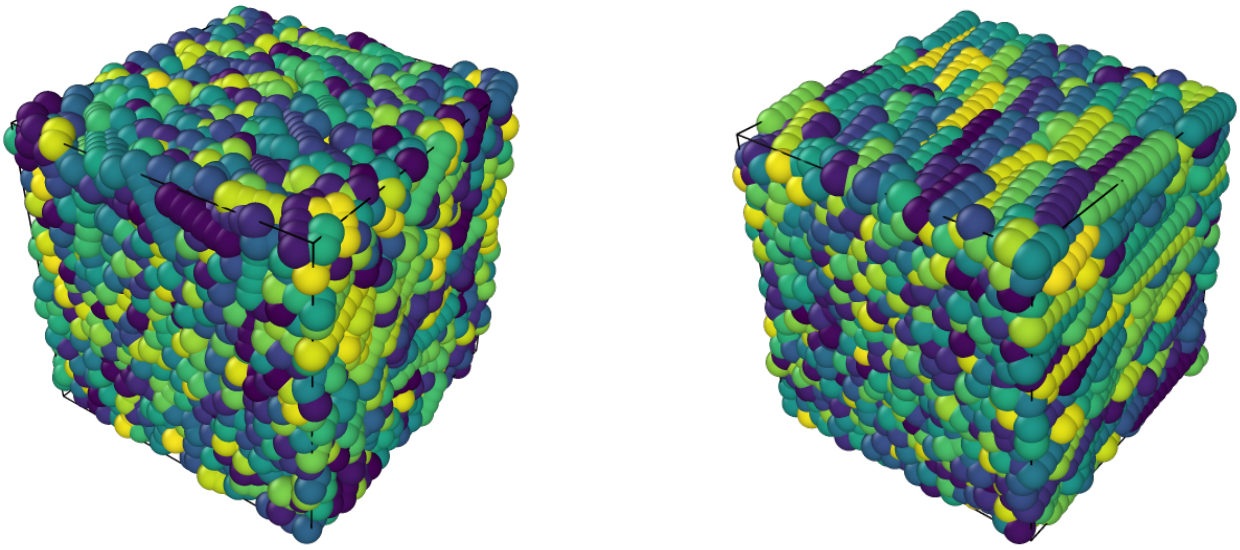

(a) *Liquid State* **(b)** *Nematic State*

Figure 1: *Comparison between phase appearance, before an after the nematic phase transition. Note the common alignment in the nematic phase, without positional order.*

This phase transition is most easily observed through a jump in the pressure of the system. The equilibrium pressure at various volume fractions is plotted in Figure 2, displaying a steep change around the critical volume fraction. It is predicted that this curve would flatten out when extended over sufficiently long regions, however in this system the phase transition occurs too close to the maximal volume fraction for this to be observed.

The evolution of pressure is displayed as the system equilibrates after each shrinking stage in Figure 3. It is particularly notable here that pressure is expected to be constant under the nve ensemble (given the additional presence of a temperature thermostat), and this is indeed observed at low volume fractions (corresponding to smaller values of 'mix_steps' - the shrinking time). However, there is a clear phase transition occurring during the fourth shrinking section, with a decrease in the pressure of the red curve. The phase transition may not be complete after this step, hence the smaller pressure change in the next equilibration stage (following further shrinking), given in the purple line.

It is a time average of these curves that gives the pressures used in Figure 2, although only the last 10% of the curve is used, where the system is assumed to have finished equilibrating, to give an accurate measurement of temperature. It should be noted however that the pressure is hard to define in molecular level systems like this, and is subject to significant fluctuations due to its low magnitude. This meant that the curves in 3 have been smoothed significantly, and are subject to variations much greater than their net change, on the order of ± 0.1 natural units.

It is for this reason that an alternative method to quantify the phase change here is sought. Traditionally the order parameter is used for the nematic phase change, detailed in Section 1.1. This was calculated (approximating the local director as the mean molecular axis) and plotted against volume

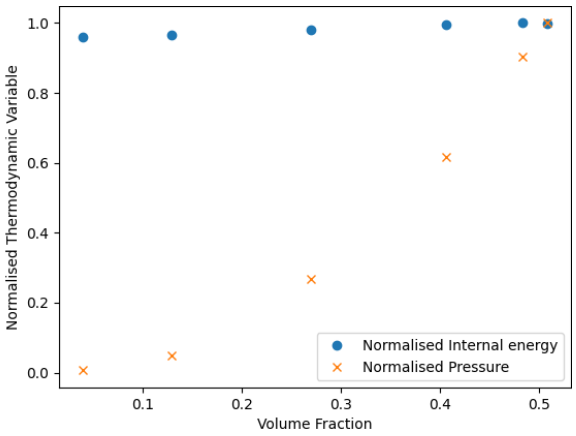

Figure 2: *Evolution of thermodynamic variables over time; change in pressure corresponds to phase transition.*

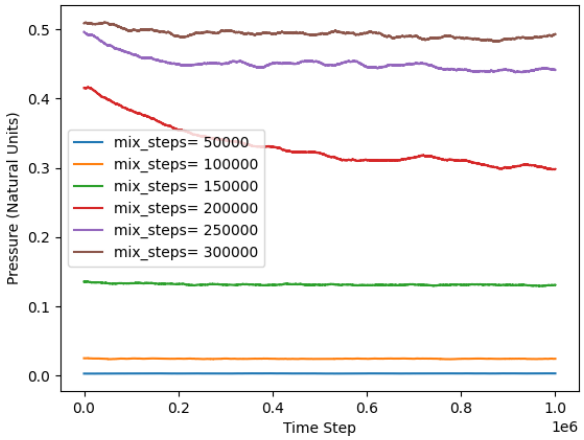

Figure 3: *Pressure evolution when system is equilibrating; the change in the red curve denotes a phase transition over this run.*

fraction in Figure 4. It should be noted that the absolute value of the order parameter is plotted here, as negative values were observed.

Further work here will extend this to an oblong simulation region, to aid the formation of ordered phases.

2.2 Oblong Simulation Region

Typically, the formation of ordered phase structures such as nematic or smectic phases is impeded by the edge effects of the box; the periodic boundary conditions here can destabilise the formation of ordered phases if the simulation dimensions are not an integer multiple of the molecule dimensions. (For example, when forming a smectic phase the molecules cannot line up fully in columns and must overlap at the edges of the box.)

This effect is mitigated by increasing the volume of the simulation box, as the overlapping regions form a smaller proportion of the overall structure (and this overlap may be distributed further to reduce the energy cost). We typically aim for a simulation region 5/6 larger than the molecular dimension. However, a larger simulation regions comes with associated computational costs, as a greater number of molecules are required to achieve the same volume fraction.

These costs can be reduced by breaking the symmetry of the system; we may be introduce a long axis in our simulation region to generate an oblong box. Ordered phases will preferentially form along this long axis, as the energy costs associated with the boundaries are reduced. In this way the number of particles required to 'fill' the box (i.e. achieve the desired volume fraction) is minimised, while retaining the longer simulation axis for ordered phase formation.

The simulation region is therefore adjusted to have a 3:1:1 aspect ratio, with the same time steps as used previously.The final phase structure formed depicted in Figure 5, and displays multiple regions of nematic phase with differing directors. The origin for this phase structure is unknown, but introduces complexity when identifying the critical volume fraction of the phase transition.

Further long-time simulations, with 18 shrinking sections of 25000 steps and 500,000 equilibration steps between each one, were conducted to identify the phase transition more accurately.

Again thermodynamic variables have been recorded over time here. It is particularly telling that the points cluster at high pressures in Figure 6; this indicates that we are approaching the maximal volume fraction and further compression is not possible here, hence it is unlikely we will observe this section of the graph levelling off.

A quasi-discrete change in order parameter is observed clearly in this system as the volume fraction increases, depicted in Figure 7. Again smoothing is required to obtain this order parameter, and the absolute value must be taken to avoid negative values. These suggest that mean value approach to

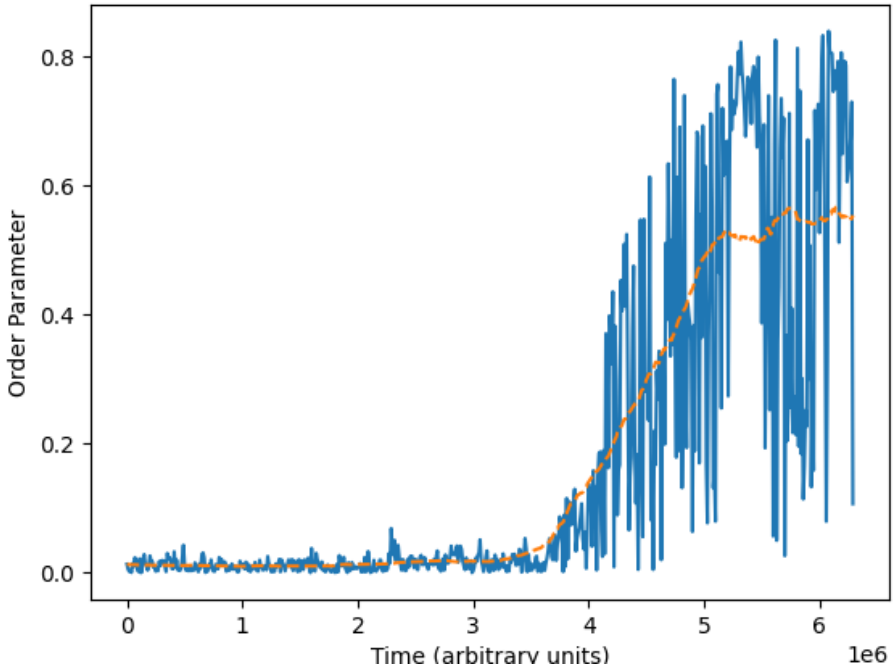

Figure 4: *The evolution of the order parameter over time for the rigid rod system depicted in blue. A rolling average (calculated over a uniform window of 500 steps) is superimposed in red here to display the overall increase in this value, and the distinct change around 4.5 million steps*

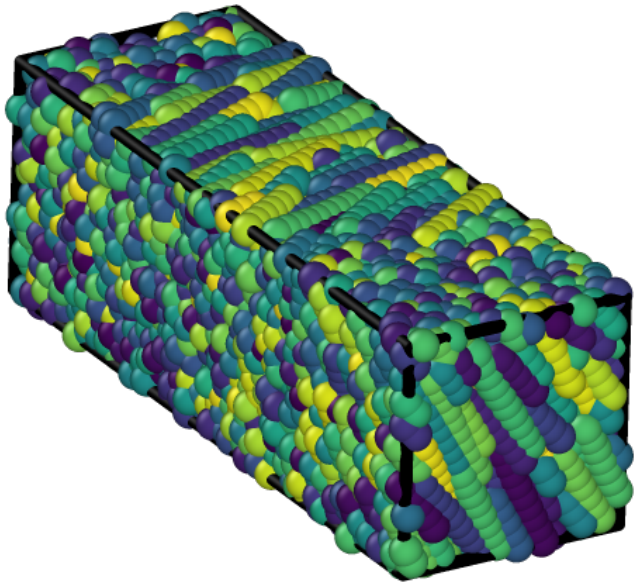

Figure 5: *The ordered phase formed in the oblong simulation region; note the two different sections of nematic phase in the foreground and background of the image, with varying local director orientations.*

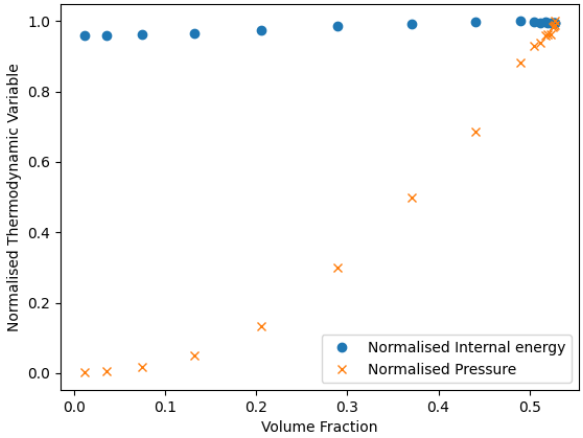

Figure 6: *Evolution of thermodynamic variables over time; change in pressure corresponds to phase transition. Note the cluster of points at high pressures corresponding to the limit of maximal volume fraction.*

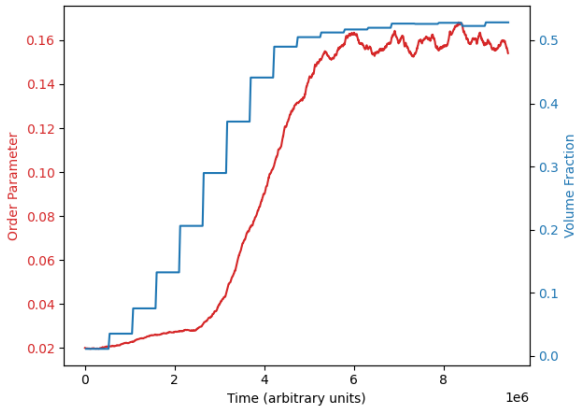

Figure 7: *Evolution of the order parameter and volume fraction over time; note the steep change in order parameter at median times, and the subsequent levelling off suggesting a new phase has been reached.*

calculate the local director may not be valid, and a more advanced method will be implemented for future simulations.

We may introduce the alternative order parameter (from Eppenga et al.) introduced in Section 1.1, to produce the phase curve in Figure 8. It should be noted that the increase in order parameter is much steeper in this new formulation, and better defines the phase transition. However, the bigger difference is within the amount of data-processing required; the need for curve smoothing (via a uniform-window rolling average) is significantly reduced, and no negative values are now obtained.

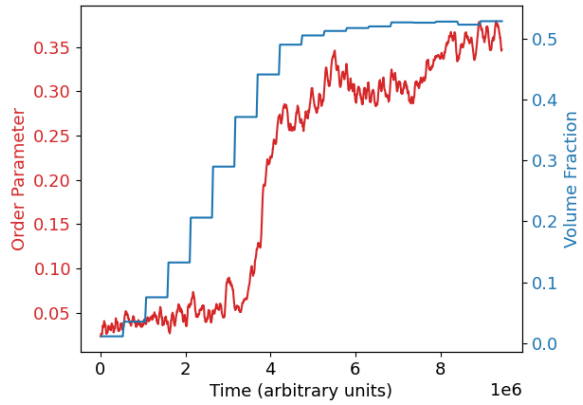

Figure 8: *Evolution of the order parameter and volume fraction over time for particles with an aspect ratio = 10; note the even steeper change in order parameter with minimal noise at median times.*

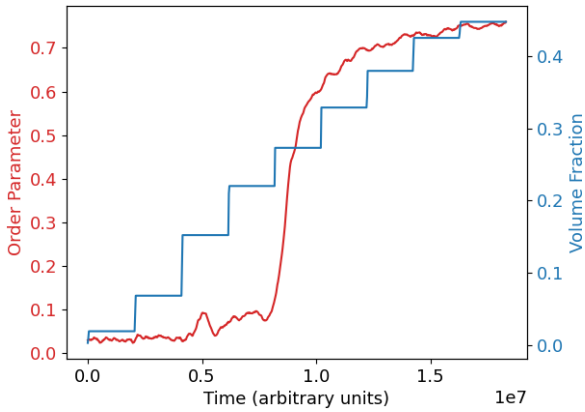

Figure 9: *Evolution of the order parameter for longer particles, with an extended aspect ratio = 16. Note the phase transition occurs at a lower volume fraction here.*

The validity of this method (and Onsager theory in general) may be verified through variation of the aspect ratio of the particles considered. I considered two cases here; the first was that of half length rods, with an aspect ratio of 5. This was in response to data from my supervisor which suggested a phase transition may occur here with a volume fraction of 50%; despite Onsager's prediction that this would require a volume fraction of 0.8 (higher than can be physically achieved with sphere-based particles due to their limited packing efficiency of 74%). My simulations seems to support Onsager's theory; I was only able to achieve a maximal volume fraction of 56% with no formation of an ordered phase occurring.

I also considered rigid rods formed of 16 adjacent spheres, which therefore are predicted to undergo a nematic phase transition at the critical volume fraction of 25%. Figure 9 displays the evolution of the order parameter for this system, and is in agreement with this theoretical prediction.

2.3 Expanding Simulation Region

In this section, I introduce simulations ran 'in reverse' - i.e. starting from a perfectly ordered (crystalline) phase, and then expanding the simulation region to observe the introduction of disorder. This is particularly important to demonstrate the validity of the nematic phase transition we have previously observed when shrinking the simulation region, and particularly that it was observed at equilibrium. This is because non-equilibrium effects will manifest themselves as hysteresis here; i.e. the 'backwards' phase transition will not occur at the same critical volume fraction as the 'forwards' (i.e. reducing volume fraction) transition.

The expanding simulation region is controlled by the time integration of Nose-Hoover style non-Hamiltonian equations of motion on a isoenthalpic ensemble. This is specified in LAMMPS by a target pressure, and a damping term, so that the system evolves isenthalpically to achieve this. The target pressure must be lower than the system pressure for expansion to occur (and the rate of expansion is controlled by the damping term, however this has been kept constant from previous simulations). It is also worth noting that a langevin thermostat is employed here to ensure the temperature of the system is conserved during this process.

As expected, we observed a nematic phase transition over the critical volume fraction of 0.4 in this system. We also observed a second phase transition in Figure 10, that we believe corresponds to the smectic-nematic phase transition, however further work is required to verify this (such as calculation of a more appropriate order parameter for this phase transition).

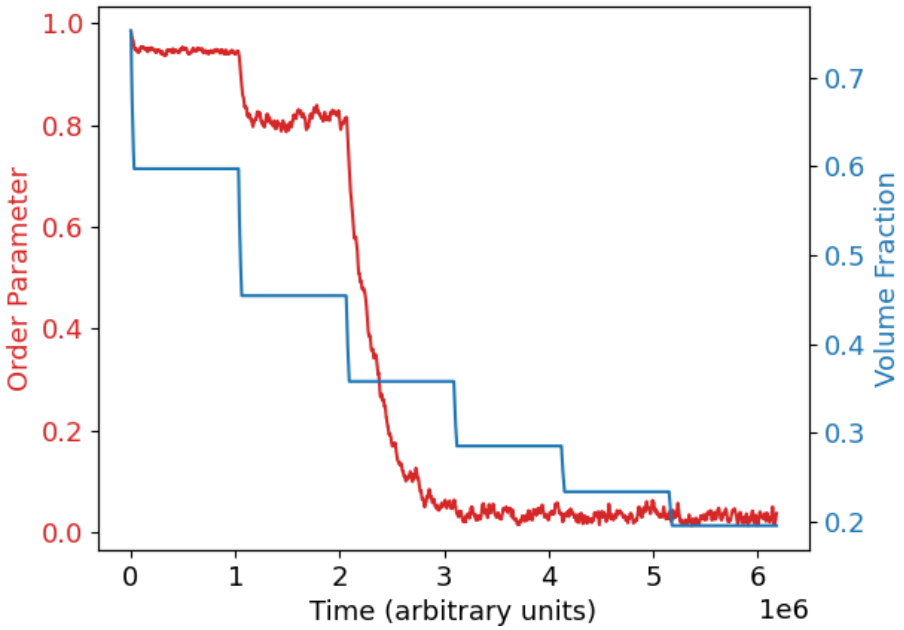

Figure 10: *Evolution of the order parameter and volume fraction over time; note the two phase transitions observed (corresponding to steep changes in the order parameter).*

References

[1]R. Eppenga and D. Frenkel, "Monte carlo study of the isotropic and nematic phases of infinitely thin hard platelets", Molecular Physics **52**, 1303–1334 (1984).